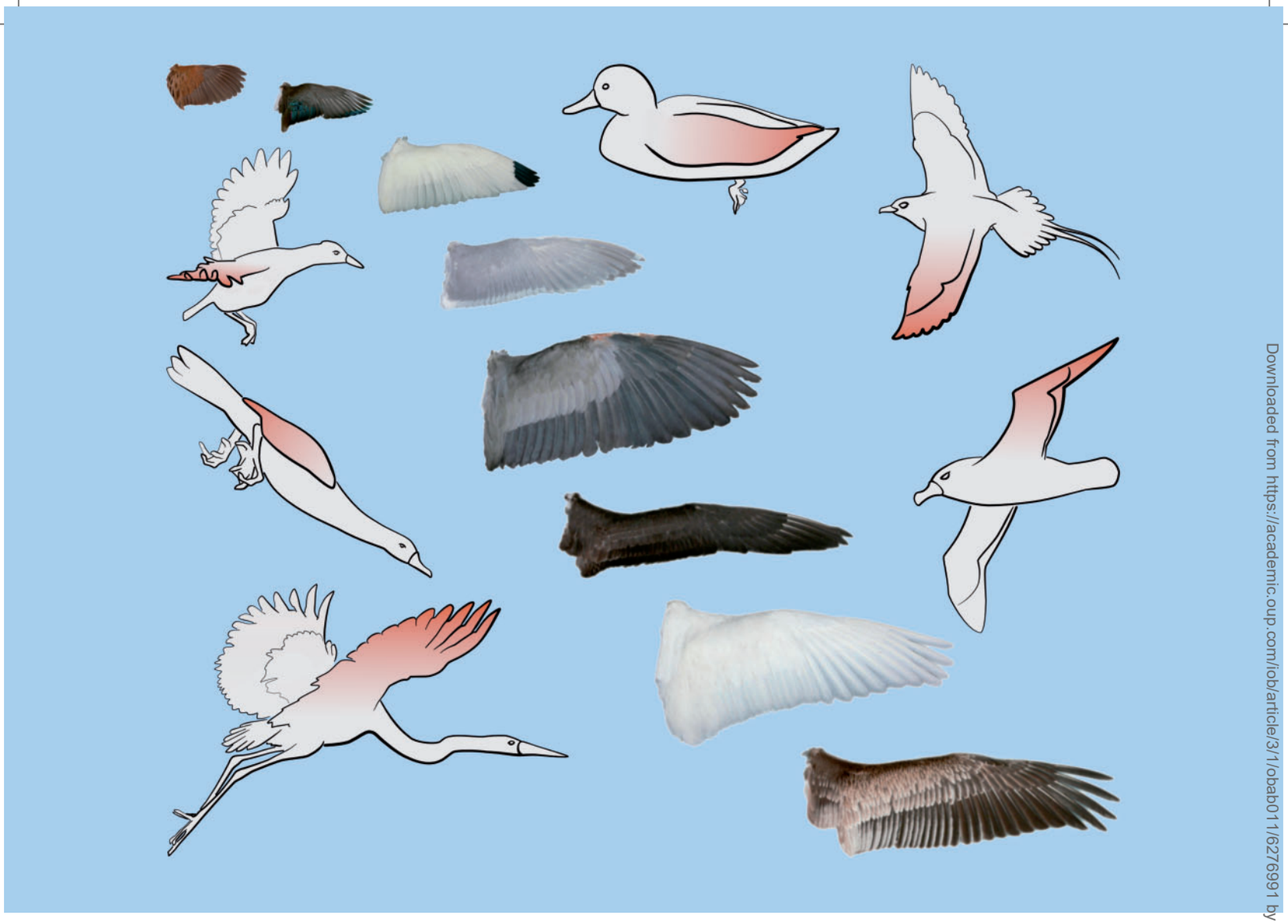

Integrative Organismal Biology

A Journal of the Society for Integrative and Comparative Biology

academic.oup.com/icb

OXFORD UNIVERSITY PRESS

Integrative Organismal Biology

Integrative Organismal Biology, pp. 1–20
doi:10.1093/iob/obab011

A Journal of the Society for Integrative and Comparative Biology

RESEARCH ARTICLE

Wing Shape in Waterbirds: Morphometric Patterns Associated with Behavior, Habitat, Migration, and Phylogenetic Convergence

Stephanie L. Baumgart ,*[1] Paul C. Sereno*,† and Mark W. Westneat*,†

*Department of Organismal Biology and Anatomy, University of Chicago, 1027 E, 57th St, Chicago, IL 60637, USA;
†Committee on Evolutionary Biology, University of Chicago, 1027 E, 57th St, Chicago, IL 60637, USA

[1]E-mail: slbaumgart@uchicago.edu

Synopsis Wing shape plays a critical role in flight function in birds and other powered fliers and has been shown to be correlated with flight performance, migratory distance, and the biomechanics of generating lift during flight. Avian wing shape and flight mechanics have also been shown to be associated with general foraging behavior and habitat choice. We aim to determine if wing shape in waterbirds, a functionally and ecologically diverse assemblage united by their coastal and aquatic habitats, is correlated with various functional and ecological traits. We applied geometric morphometric approaches to the spread wings of a selection of waterbirds to search for evolutionary patterns between wing shape and foraging behavior, habitat, and migratory patterns. We found strong evidence of convergent evolution of high and low aspect ratio wing shapes in multiple clades. Foraging behavior also consistently exhibits strong evolutionary correlations with wing shape. Habitat, migration, and flight style, in contrast, do not exhibit significant correlation with wing shape in waterbirds. Although wing shape is critical to aerial flight function, its relationship to habitat and periodic locomotor demands such as migration is complex.

Résumé La forme de l'aile joue un rôle essentiel dans le vol chez les oiseaux et les autres animaux présentant un vol actif. Il a été démontré que cette dernière est corrélée aux performances de vol, à la distance de migration et à la biomécanique générant de la portance pendant le vol. La forme de l'aile et la mécanique du vol chez les oiseaux sont également associées au comportement alimentaire et au choix de l'habitat. Notre objectif est de déterminer si la forme de l'aile chez les oiseaux aquatiques, un assemblage fonctionnellement et écologiquement diversifié uni par leurs habitats côtiers, est corrélée à divers traits fonctionnels et écologiques. Nous nous sommes appuyés sur des techniques de morphométrie géométrique appliquées aux ailes déployées d'une sélection d'oiseaux aquatiques afin de mettre en évidence un lien évolutif entre la forme des ailes, le comportement alimentaire, l'habitat et les mouvements migratoires. Nous avons trouvé des preuves concrètes de l'évolution convergente des formes d'ailes à fort et faible allongements dans plusieurs clades. Le comportement alimentaire présente également de fortes corrélations évolutives avec la forme des ailes. L'habitat, la migration et le style de vol, en revanche, ne présentent pas de corrélation significative avec la forme de l'aile chez les oiseaux aquatiques. Bien que la forme de l'aile soit essentielle au vol, sa relation avec l'habitat et les exigences locomotrices périodiques telles que la migration reste complexe.

Introduction

Wing shape has long been known to exhibit a strong correlation with a generalized description of aerodynamic performance: long, narrow wings (high aspect ratio [AR]) characterize large-bodied gliding and soaring organisms, whereas short, broad wings (low AR) characterize smaller-bodied organisms with more maneuverable flight (Norberg 1990; Tobalske 2007; Alexander 2015). This general correlation between wing shape and aerodynamic function has also been found in every group of aerial or aquatic powered fliers, including cephalopods, insects, fishes, pterosaurs, and bats, and has often been applied to airfoil design in mechanized flight (Da Vinci 1505; Norberg 1990, 1995; Hansen 2003; Lentink and Biewener 2010; Martin-Silverstone et al. 2020). Despite the extensive body of work on bird flight and wing shape, we are only beginning to

understand the complexity of biological wings, the relationship between their form and their function, and their evolutionary history.

Previous work has shown a strong relationship between avian wing shape and various aspects of flight function. AR has a significant relationship with maneuverability, rapid takeoff, and efficient gliding (Hartman 1961; Greenewalt 1975; Norberg 1990). Wingtip shape has proven to be significant with regards to dispersal ability, takeoff, and flight performance, and relative migration distance within species or between closely related species (Mulvihill and Chandler 1990; Lockwood et al. 1998; Combes and Daniel 2001; Swaddle and Lockwood 2003; Brewer and Hertel 2007; Claramunt et al. 2012; Minias et al. 2015). Wang and Clarke (2014, 2015) discovered that wing bone shape and wing outlines have a strong phylogenetic signal when examined in an evolutionary context; wing shape was more closely associated with clade membership than flight style. In addition, recent work across birds has linked wing length and beak morphology to feeding behaviors and ecological habitats (Pigot et al. 2020). These large-scale analyses show convergence as a common evolutionary pattern across birds, underscoring the need to carefully assess avian morphological traits against the phylogenetic and ecologic background of birds selected for the study.

Waterbirds comprise a diverse assemblage for exploring patterns of morphological and ecological diversity. They include water-adapted species from 3 clades: Aequiornithines (diving birds, wading birds, and shorebirds), Gruiformes (containing rails and cranes), and Anseriformes (ducks and geese) (Prum et al. 2015). With sufficient ornithological interest for their own focus group (e.g., Waterbird Society), waterbirds have been subject to extensive research including recent exploration of the genetic basis underlying interdigital webbing in their feet (Tokita et al. 2020). Waterbirds, known conclusively now to be representatives of at least 3 phylogenetic assemblages, are nonetheless united ecologically by their proximity to, and dependence on, aquatic or nearshore habitats that has led to convergence in morphology, trophic strategy, and locomotor behavior. Recent work shows that waterbird wing shapes are diverse, occupying roughly half of total avian wing shape space (Wang and Clarke 2014, 2015). These studies, among the first to analyze avian wing shape within phylogenetic context, demonstrated that some traditional, functional, and ecological variables showed little correlation with wing shape. This result runs counter to the idea that form and function are correlated. Thus, exploration of wing shape among the diversity of waterbirds may yield unexpected insights in the relationship between structure and function.

We began with the hypothesis that using landmark-based geometric, rather than simple linear, morphometrics to capture waterbird wing shape would yield clearer relationships to important ecological traits. And given that no single variable fully captures the complexity of avian lifestyle, we tested several: flight style, foraging behavior, habitat, migratory status, and migratory status categorized by geographic location. Flight style has previously been used to describe the wingbeat pattern used in horizontal flight, that is, frequent flapping versus gliding (Viscor and Fuster 1987). Foraging behavior better captures the range of different behaviors that may require more or less agility, for example, plunge diving versus dabbling. Habitat categories often reflect differences in air currents or foliage density, which again would draw upon wing function. Finally, migration variables are used here to capture how much a bird requires long distance migratory flights, and determine whether long migratory distances over land rather than ocean results in any wing shape differences.

Our central aim is to explore the relation between wing metrics and a variety of ecological variables waterbirds, which exhibit diverse behaviors in a range of habitats. We test the hypothesis that wing shape and foraging behavior are strongly correlated (Webb 1984; Higham 2007) and test the strength of the correlation between wing shape indices and migratory patterns. Using geometric morphometric data in the context of a well-resolved phylogeny (Hackett et al. 2008; Jetz et al. 2012), we also examine biomechanical traits such as the distribution of wing area (WA), wing loading (WL), and wing AR. Finally, we look anew at phylogenetic convergence of wing shape in the light of an integrated phylomorphospace and comparative approach.

Materials and methods

Specimen selection, phylogeny, and ecological data sources

We analyzed wing images for 136 species of waterbirds from 8 clades to search for correlation with ecological or behavioral traits (Supplementary Table S1). A diversity of wing shapes is represented (Fig. 1). Penguins are excluded because their wing feather morphology is too divergent for many of the measurements in this study (e.g., no clear distinction between primary, secondary, and covert feathers) and because previous work has shown their wing outlines differ markedly from that of other birds (Wang and

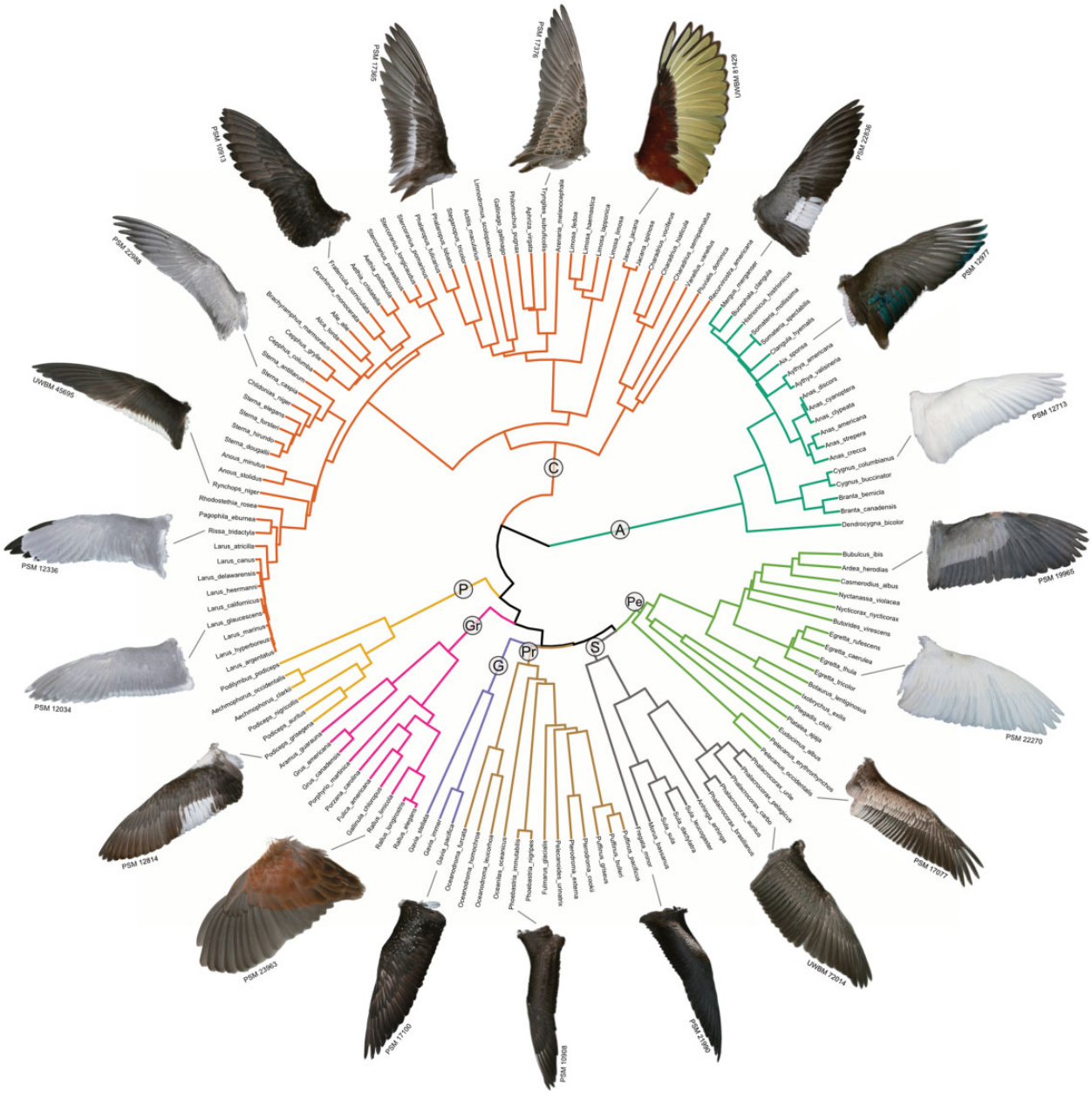

Fig. 1 Waterbird wing shapes across the phylogeny with color-labeled clades: A, Anseriformes; C, Charadriiformes; P, Podicipediformes; Gr, Gruiformes; G, Gaviiformes; Pr, Procellariiformes; S, Suliformes; Pe, Pelecaniformes. Images reproduced with permission from the Puget Sound Wing and Tail Image Collection and the Burke Museum of Natural History and Culture.

Clarke 2015). Included species all are documented by an adult wing (dorsal view) in the Wing and Tail Image Collection of the University of Puget Sound's Slater Museum of Natural History (2011). All included wing images are preserved in the standard "spread wing" position.

Our phylogeny follows Pigot et al. (2020) in the use of the avian molecular tree of Jetz et al. (2012), the latter based on the earlier phylogenetic tree of Hackett et al. (2008). One thousand full molecular trees from the Hackett Sequenced Series were downloaded from BirdTree.org. A maximum credibility tree was created from these 1000 trees with median node heights using TreeAnnotator from BEAST (Drummond and Rambaut 2007). The resulting tree contained a single negative branch length, which was converted to a branch length of 0.01. The tree was imported into R and pruned to our species with the *drop.tip()* function in the *ape* package (Paradis and Schliep 2019) for subsequent use in phylogenetic analyses.

We scored our sample of 136 waterbirds for body mass, phylogenetic relationships, and a suite of ecological traits including foraging behavior, habitat,

and migration. For body mass, we accessed data in Dunning (2007). We gathered ecological trait data from various traditional and recent compilations. "Flight style" came from Viscor and Fuster (1987) with species in our analysis coded according to their clade-level assignments. "Foraging behavior" was adapted from the "All About Birds" website (Cornell Lab of Ornithology 2015), *The Birder's Handbook* (Ehrlich et al. 1988), and the Animal Diversity Web (Myers et al. 2020) (see "Terminology" in Supplementary text for the list of terms). All terms were taken from the Cornell Lab of Ornithology, except "aerial hunter," which we use here to describe birds that hunt on the wing. Jaegers and frigatebirds, for example, prey on other birds in flight, and petrels often catch food on the wing rather than diving (Cornell Lab of Ornithology 2015). In both of these cases, significant time is spent in the air to catch prey. "Foraging niche" was defined and logged following Pigot et al. (2020). As we found no substantive differences between foraging niche and foraging behavior (Supplementary Fig. S2), we used foraging behavior. "Habitat" data came from the Cornell Lab of Ornithology (2015), *The Birder's Handbook* (Ehrlich et al. 1988), and the Animal Diversity Web (Myers et al. 2020).

"Migratory status" (full migrant, partial migrant, and nonmigrant) was obtained from *BirdLife International* (2020). Most species in this compilation were logged as full migrants or non-migrants. A single species, *Phalacrocorax carbo* (great cormorant), was registered as a third category, "partial migrant," because only part of the population migrates. The majority of waterbirds have geographic ranges that were scored as either "continent-based" or "oceanic" using range maps from *BirdLife International* (2020). As a result, we scored our waterbirds for an additional variable that combines migratory status with geographic location. Only 5 species ranged across both continental and oceanic geography, and we scored these as "mixed range." We combined these data with migratory status to generate our variable "Migration+Location" (i.e., continental migrant, continental nonmigrant).

Digitization

To capture wing shape, wing images were digitized with a mixture of homologous and sliding semi-landmarks (Fig. 2A for wing anatomy; Fig. 2B for numbered landmarks). The trailing edge of the coverts was also included in wing shape, because overall covert shape was found to contribute significantly to wing shape disparity (Wang and Clarke 2015). The R package *StereoMorph* (Olsen and Westneat 2015; Olsen and Haber 2017) was used to digitize the images. Homologous landmarks (Fig. 2B, larger red circles) include the anteroproximal point (approximate location of the humeral head), the anteriormost part of the wrist, the distal tips of the first 5 primary flight feathers, the division between primary and secondary flight feathers, the last secondary flight feather, the distalmost primary greater covert tip, the division between the primary and secondary greater coverts, and the last secondary greater covert. Six curves of sliding semi-landmarks (Fig. 2B, smaller yellow circles) were created at the anterior edge of the wing (humeral head to wrist, wrist to distal tip of first primary flight feather), the posterior edge of the flight feathers (tip of fifth primary flight feather to tip of last primary flight feather and tip of last primary flight feather to tip of last secondary flight feather), and the posterior edge of the greater coverts (distalmost tip of primary coverts to tip of last primary covert, tip of last primary covert to tip of last secondary covert). These points create the dataset for the whole-wing morphospace, subsets of which were used to calculate additional variables and morphospaces.

Wing shape measurements and functional metrics

Wingspan, wing length, AR, WA, WL, and pointedness of the wingtip (for symbols, see Table 1) are the most commonly used wing metrics for comparative functional analysis (Ellington 1984; Norberg 1990). We followed the terminology used in Norberg (1990): *wingspan, b*, is the distance between wingtips; *wing length, l_w*, is the distance from the shoulder joint to wingtip; *armwing length, l_{aw}*, is the distance between the shoulder and wrist joints; and *handwing length, l_{hw}*, is the distance between wrist joint and wingtip (Fig. 2A). It is worth noting that ornithologists have often used "wing length" as the measure from the wrist joint to the wingtip (equivalent to l_{hw}), because that has been the easiest measure to get from a museum specimen with a folded wing (Greenewalt 1962). Because we used spread wings, we can distinguish between the different regions of the wing.

Traditionally, AR is wingspan divided by mean chord, because the chord of a bird wing changes significantly over its length. However, most recent studies measure single-wing AR, as wing length squared divided by WA (Norberg 1990). We followed that convention here as $\mathrm{AR} = \frac{l_w^2}{S_w}$. We also developed an AR slope metric ("AR slope") using wing length and a series of 5 incrementally more

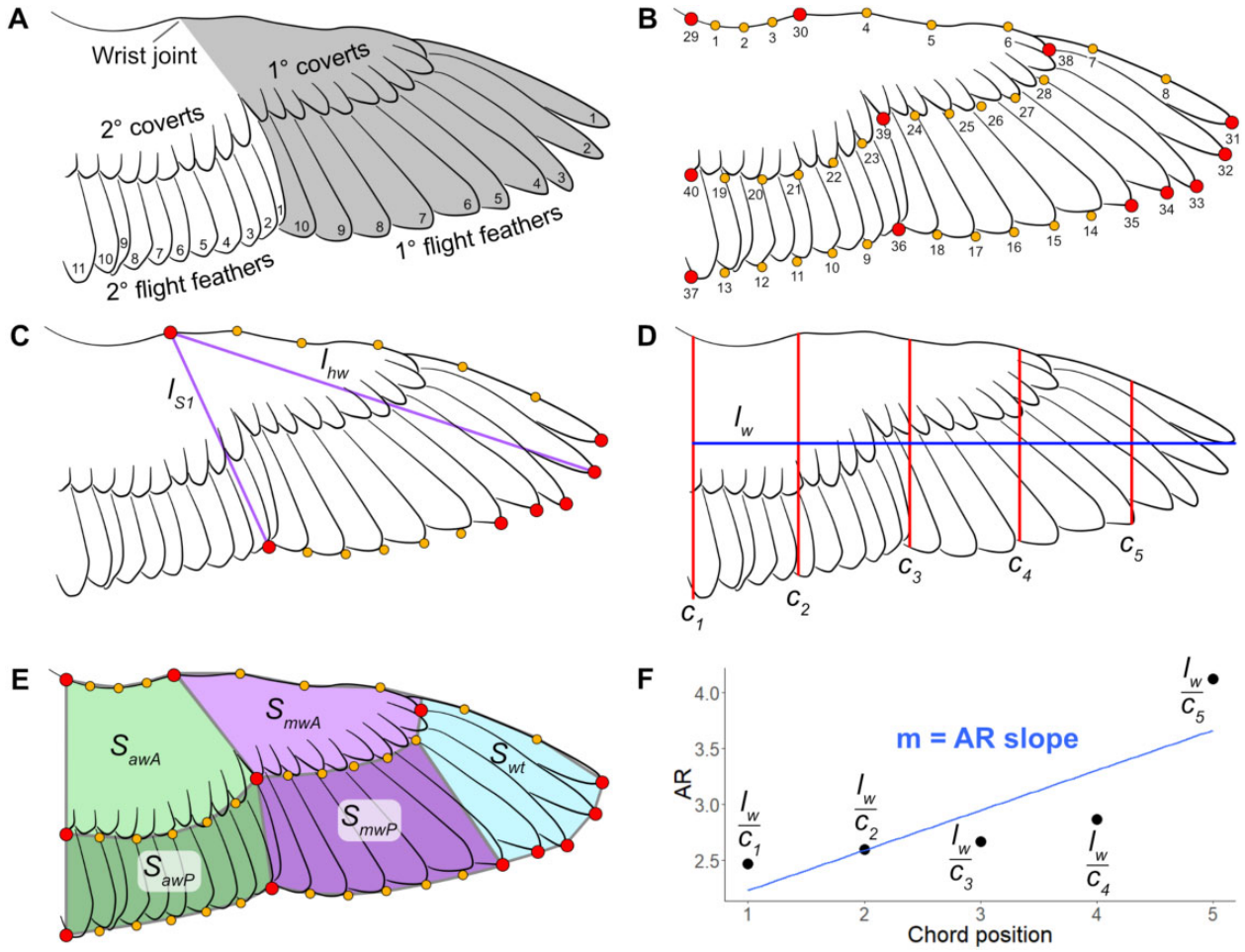

Fig. 2 Landmark protocol for wings. **(A)** Anatomy of a bird wing, handwing—gray portion, armwing—white portion; **(B)** Numbered homologous landmarks (red) and sliding semi-landmarks (yellow); **(C)** Subset of landmarks used for handwing morphospace, and measurements taken for handwing index calculations (purple, l_{S1} and l_{hw}); **(D)** Wingspan (blue, l_w) chords (red, C_1–C_5) for AR distribution analysis; **(E)** WA segments: anterior armwing (light green, S_{awA}), posterior armwing (dark green, S_{awP}), anterior midwing (light purple, S_{mwA}), posterior midwing (dark purple, S_{mwP}), wingtip (light blue, S_{wt}); **(F)** Calculating slope for AR distribution of a wing.

Table 1 Variables and abbreviations for wing and aerodynamic metrics (adapted from Norberg 1990)

AR = aspect ratio	l = length	Mg = body weight	S_w = area of one wing
b = wingspan, wingspread	l_{aw} = armwing length	m_w = mass of one wing	T_i = wingtip-shape index
c = wing chord	l_{hw} = handwing length	S = airfoil or WA	T_l = wingtip-length ratio
$\bar{c}$ = mean wing chord	l_w = wing length	S_{aw} = armwing area	T_s = wingtip-area ratio
g = acceleration of gravity	M = body mass	S_{hw} = handwing area	WL = wing loading

distal chords to calculate an AR series along the wing. These points generated a linear regression (Fig. 2F), from which was derived the AR slope. This metric measures the degree that AR changes along the length of the wing.

Airfoil area (S) refers to the lift-generating surface of an object (Table 1) (Norberg 1990). Single-WA (S_w) refers solely to the area of one wing (Norberg 1990). Armwing area (S_{aw}) is the area of the wing between the shoulder and wrist joints, which extends across the secondary feathers (Fig. 3A), and handwing area (S_{hw}) is the area of the wing between the wrist joint and the wingtip, which extends across the primary feathers (Fig. 3A) (Norberg 1990). WL ($\frac{Mg}{S}$) is a measure of the force of body weight placed per unit of WA (Norberg 1990). Pennycuick (2008) noted that WL needs to be calculated using total airfoil area (S), which includes the area of both

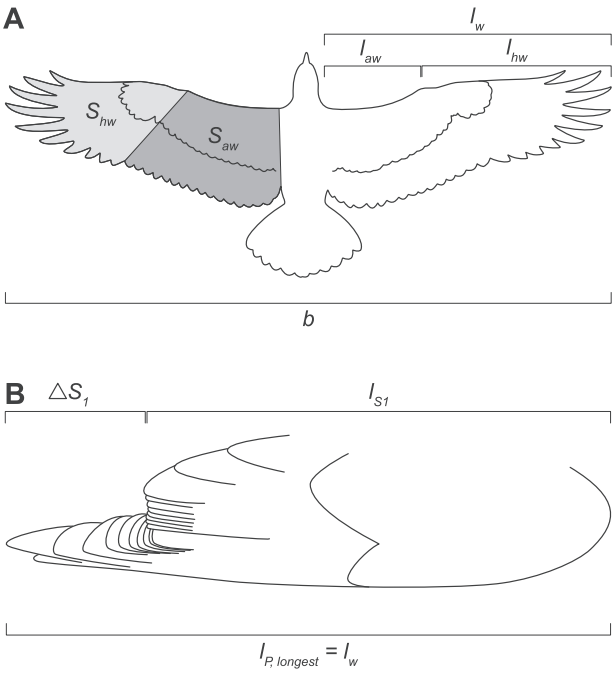

Fig. 3 Wing measurements associated with flight performance. (**A**) Based on definitions in Norberg and Rayner (1987) and Norberg (1990). (**B**) Measurements on folded wings for Kipp's index (Lockwood et al. 1998), illustration adapted from Sibley (2018). Abbreviations: *b*, wingspan; *l*, length; *S*, area; ΔS_1, distance between longest primary and first secondary flight feathers.

wings and the body. This area represents the portion of the bird that is contributing to lift while gliding. Norberg and Rayner (1987) examined data from many birds and bats and found that the body area is ~20% of combined WA. Because our dataset is composed of single wings, we approximated WL as $\mathrm{WL} = \frac{Mg}{2S_w + (2S_w \times 0.2)}\ \mathrm{N{\cdot}m^{-2}}$.

Handwing pointedness has been linked to flight performance and dispersal ability (Lockwood et al. 1998; Claramunt et al. 2012). "Kipp's distance" (ΔS_1) has been defined as the distance between the longest primary and secondary flight feathers, though has since changed to being the distance between the longest primary flight feather and first secondary flight feather: $l_w - l_{S1}$ (Kipp 1959; Lockwood et al. 1998; Claramunt et al. 2012; Pigot et al. 2020; Sheard et al. 2020), which is readily measured on the folded wings of museum specimens (Fig. 3B). "Kipp's index" (I_K), or the "handwing index" (HWI), is a commonly used metric for wingtip shape. This index is often calculated as a proportion of Kipp's distance against the traditional wing length measurement: $I_K = \frac{l_w - l_{S1}}{l_w} \times 100$ (Fig. 3B) (Lockwood et al. 1998; Baldwin et al. 2010).

WingMorph app for calculating functional metrics

We developed a Mac Xcode app called *WingMorph* (free for download; http://www.github.com/mwestneat/WingMorph) to calculate functional metrics for bird wings. The app imports the two-dimensional wing landmarks, from which it computes functional metrics (wing spans, chords, ARs, HWI, regional WAs, and total WA; Fig. 2C–E) that are output as a trait matrix (.csv) file. The full set of wing metrics calculated for our waterbird dataset is available (Supplementary Table S2).

Morphometric analysis and phylogenetic comparative methods

The functional metric morphospace was calculated using AR, AR slope, WA, WL, and HWI. These data were size corrected by calculating the log shape ratios for WA and WL, two variables strongly affected by body size. A single geometric mean was calculated between WA and WL. Each of those variables was divided by that geometric mean, and those values were $\log_{10}$-transformed (Mosimann 1970; Price et al. 2019). Because each of the variables in morphospace use dramatically different ranges, each set of variables were z-scored for standardization before running the principal component analysis (PCA).

Geometric morphometric analysis was performed using the R packages *geomorph* (Adams et al. 2020) and *RRPP* (Collyer and Adams 2018; 2020), which included a General Procrustes analysis of coordinate data (used for standardizing landmark data in whole-wing and handwing data) and PCA to generate whole-wing and handwing morphospaces. The whole-wing morphospace was represented by the landmarks in Fig. 2B, and the handwing morphospace was represented by a subset of those landmarks outlining the handwing, from the wrist, around the wingtip, to the last primary flight feathers (circles in Fig. 2C). Wing area (WA) distribution data (calculated from polygons as presented in Fig. 2E) were analyzed using PCA using the base *prcomp()* function (R Core Team 2020). *Phytools* (Revell 2012) was used for discerning phylogenetic signal (*phylo.sig()*, Pagel's lambda) and ancestral state estimation (discrete character: *reRootingMethod()*; continuous character: *contMap()*). The equal rates (ERs) and symmetric rates models were recommended for *reRootingMethod()* (Revell 2012), and they had an equivalent log likelihood for this dataset, so the ER model was used in this analysis. *Ape* (Paradis and Schliep 2019) was used for setting up the phylogenetic tree, and *geiger* (Harmon et al. 2008) was used for phylogenetic analysis of covariance (*aov.phylo()*, 1000 simulations, Wilks test). Phylogenetic analysis of covariance (phylo-MANOVA) was done with the first 6 PCs for whole-wing morphospace data (90.9% total variance) and with the first 3 PCs for handwing

morphospace data (91.3% total variance). Data were plotted with *ggplot2* (Wickham 2016) and *plotly* (Sievert 2020), and phylomorphospaces were plotted using *ggphylomorpho* (Barr 2017). A few nonwaterbird clades among our waterbird clades (Galliformes, Strisores, Columbaves, and Inopinaves (=landbirds); following nomenclature of Prum et al. 2015) are either arboreal or ground-dwelling. These birds were excluded so they would not introduce nonwaterbird behaviors to the analyses.

Convergence in whole-wing shape among waterbirds was tested by using the R package *convevol* (Stayton 2015). We used the function *convratsig()* to test whether identified sets of tip species have converged more strongly on a region of morphospace than would be expected from that of a simulated null distribution. We used convergence measure C1, representing the proportion of the maximum distance between focal taxa that has been closed by evolution. For several larger groups of species, we also used the function *convnumsig()* to test whether the frequency of lineages independently evolving into a certain region of morphospace is significantly different from a simulated null distribution (convergence measure C5). Both tests were run with 1000 simulations. The *convnumsig()* function requires the number of species selected for comparison within a given group to be larger than the number of variables, in this case, PCs. As such, only the first 5 PCs were used for *convnumsig()* to enable tests for clusters with 6 species or more. The *convratsig()* function does not have this restriction, allowing us to use 10 PCs (~90% total variance) for clusters with 2–10 species and increase the robustness of the convergence analysis.

Results

Our geometric morphometric analysis provided new information on wing shape and wing functional metrics in waterbirds. We found that whole-wing AR, WA, WL, and body mass, are all significantly influenced by phylogenetic relationships (Supplementary Table S3). Our phylogenetic comparative analyses showed that wing shape in waterbirds is significantly associated with ecological traits, such as foraging behavior and habitat, but not with migratory behaviors. Phylomorphospace analysis revealed a strong phylogenetic pattern of repeated convergence in wing shape across waterbird clades.

Wing shape correlations with ecology and migration

Results show a wide range of wing shapes in waterbirds, from short, broad low AR wings in the rail *Rallus limicola* (AR = 1.8) to long, slender, high AR wings in the albatross *Phoebastria immutabilis* (AR = 5.8) (Figs. 4–8). Results show strong patterns of correlation between multiple wing metrics and ecological traits such as foraging behavior and habitat across the phylogeny of waterbirds. Some significant differences were found to be associated with taxonomic grouping as well, but there was no significant association of waterbird wing shape functional metrics with migratory status. Below is a summary of the functional metrics and discussion of key variables. We present the complete analysis of functional metrics and their ecological and migratory associations in the supplementary materials.

Both low and high AR wings appear to have evolved at least 5 times independently (Fig. 4B). The waterbirds with higher AR wings tend to be plunge divers and aerial hunters (Fig. 4 and Supplementary Fig. S3C), although albatrosses with very high AR wings dabble (surface skim or head submerged tipping downward) when they forage (Fig. 4). Birds with lower AR wings tend to be probers and stalkers (Fig. 4 and Supplementary Fig. S3C). Surface divers, ground foragers, and dabblers tend to have medium AR wings (Fig. 4 and Supplementary Fig. S3C).

Functional metrics plotted in morphospace suggest there exists significant overlap between major groups for foraging behavior and migration+location variables (Fig. 5). The loadings in Fig. 5A and Supplementary Table S4 show that AR, AR slope, and HWI are positively correlated and provide most of the influence for PC 1. WA and WL are also positively correlated and mostly influence PC 2. The top left (low on PC 1 and high on PC 2) has birds with low AR wings and a low HWI. Moving toward the higher PC 1 are birds with high AR wings and a high HWI. Birds with low PC 2 values do not have a notably different AR than the birds with higher PCs, but it seems there is a complex interaction with WA and/or WL to bring the species to the lower PC 2 values.

Landmark-based morphospaces of waterbird wings

Whole-wing morphospace

Whole-wing morphospace shows some clustering by clade, whereas ecological specializations distinguish species from a central cluster that includes species with various behaviors in various habitats (Fig. 6C–E). PC 1 and whole-wing AR are closely associated, boxplots following very similar trends for all phylogenetic and ecological categories (Supplementary Figs. S3A–E and S5A–E, respectively; also Supplementary

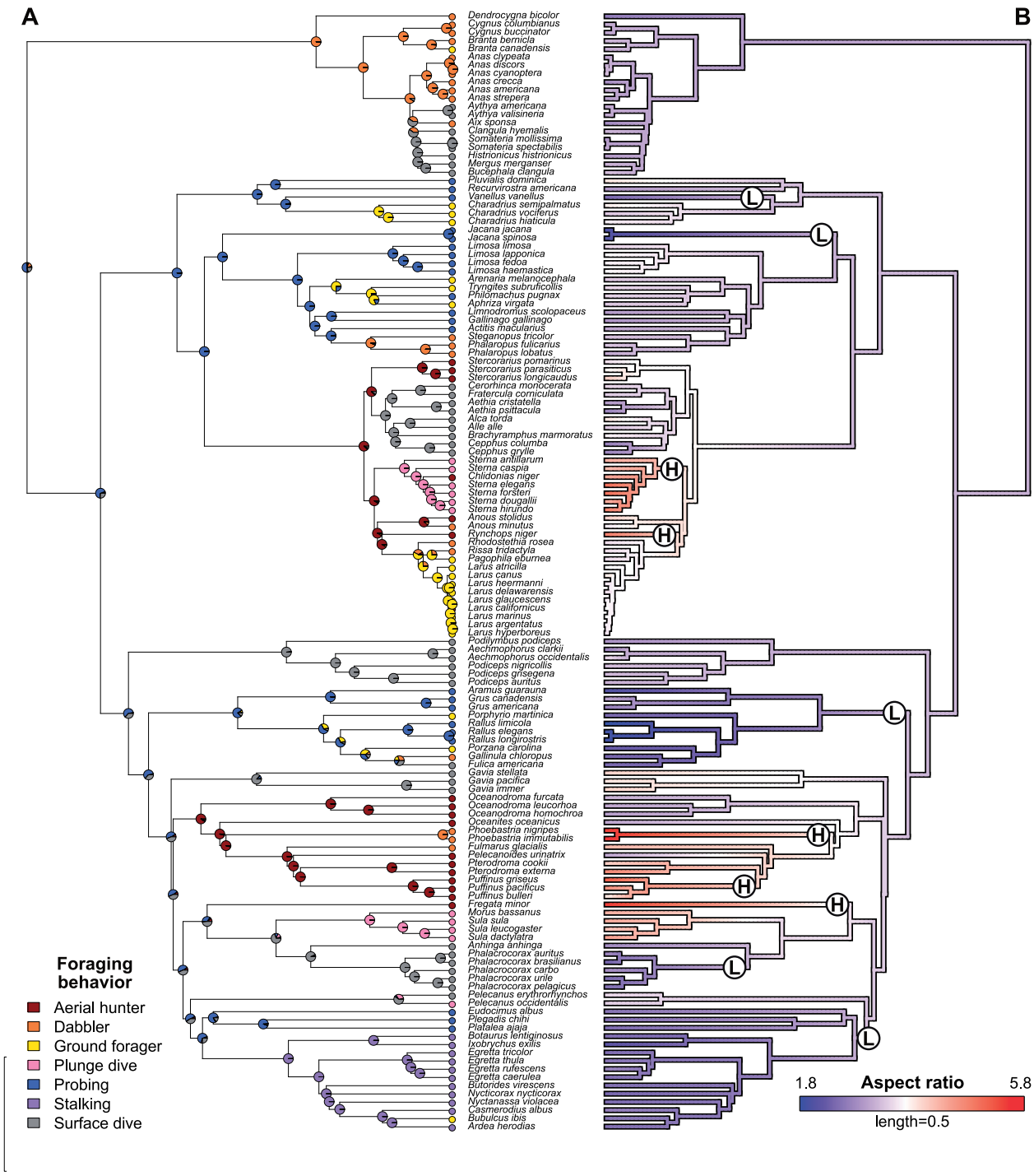

Fig. 4 (A) Ancestral state estimation of waterbird foraging behavior. **(B)** Wing AR. Abbreviations: H, evolution of high AR wings, L, evolution of low AR wings.

Fig. S6A). This trend suggests that PC 1 is driven largely by whole-wing AR, rather than body mass and WL traits (Supplementary Fig. S5F–J). PC 2 is an axis influenced strongly by the relative size of the armwing to the handwing, curvature of the leading edge of the wing (straight or curved), pointedness of the wingtip (rounded or pointed), and coverage of the primary coverts (more proximal or more distal) (Supplementary Fig. S6B). The PC 3 axis is influenced by coverage of the secondary coverts (anterior wing or extending to the trailing edge; Supplementary Fig. S6C) and the curvature of the leading edge.

Considering whole-wing phylomorphospace by taxonomic group, Anseriformes, Gaviiformes,

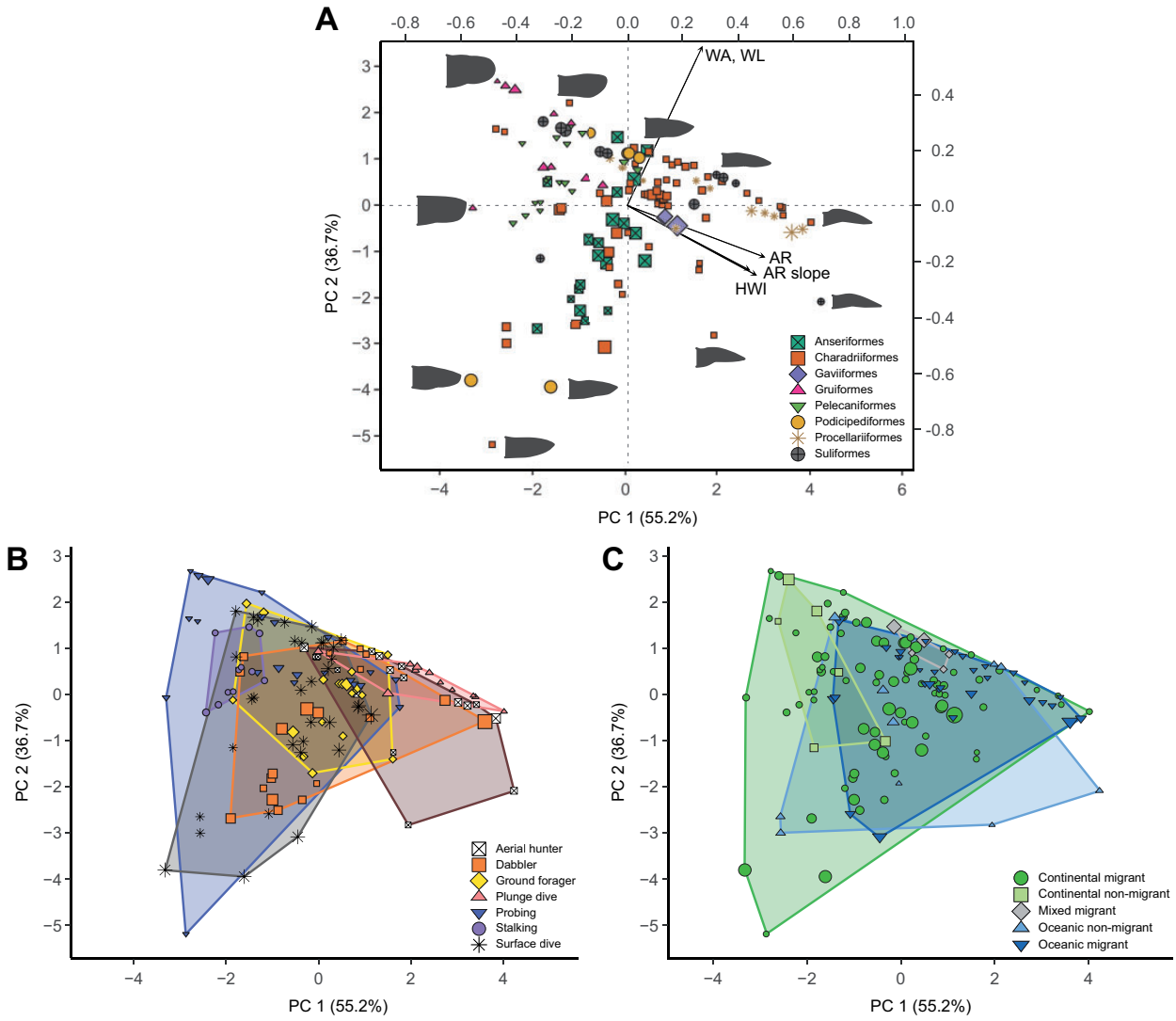

Fig. 5 Morphospace of functional metrics: AR, AR slope, WA, WL, and HWI. (**A**) colored by taxonomy and includes loading plot, (**B**) colored by foraging behavior, (**C**) colored by migration+location. WA and WL were corrected for size using Mosimann shape ratios, then all the variable distributions were standardized using z-scores before running the PCA. PCs 1 and 2 represent 91.9% of the total variance. Size of points indicates relative WL. Interactive plot in Supplementary Fig. S4.

Pelecaniformes, Podicipediformes, and Suliformes score low and Charadriiformes high on PC 2 (Fig. 6A and B). Gruiformes and Charadriiformes extend into lower PC 1 and PC 2 values, and Procellariiformes and Charadriiformes score high on PC 1 and PC 2 (Fig. 6A and B). Different flight styles feature major overlap, with only gliding/soaring birds limited to high PC 1 values (Fig. 6C). Foraging behavior is significantly correlated with whole-wing shape space (phylo-MANOVA: Wilks statistic = 0.178, $P = 0.0170$, Supplementary Table S8). Aerial hunters and plunge divers are limited to higher PC 1 values, probing birds extend to lower PC 1 values, and the other foraging behaviors are more central (Fig. 6D). The major habitat groups also feature a lot of overlap in the central region of wing morphospace (Fig. 6E), with ocean, shoreline, and a few marsh birds exhibiting higher PC 1 values. Marsh-dwelling birds also extend to lower PC 1 values. Migratory and continental birds occupy a huge range of wing morphospace (Fig. 6F and G), whereas oceanic birds (migratory and nonmigratory) are limited to higher PC 1 values (Fig. 6G).

Wing area morphospace

Like whole-wing morphospace, wing area (WA) morphospace shows a central cluster with some peripheral extensions. This analysis compares the

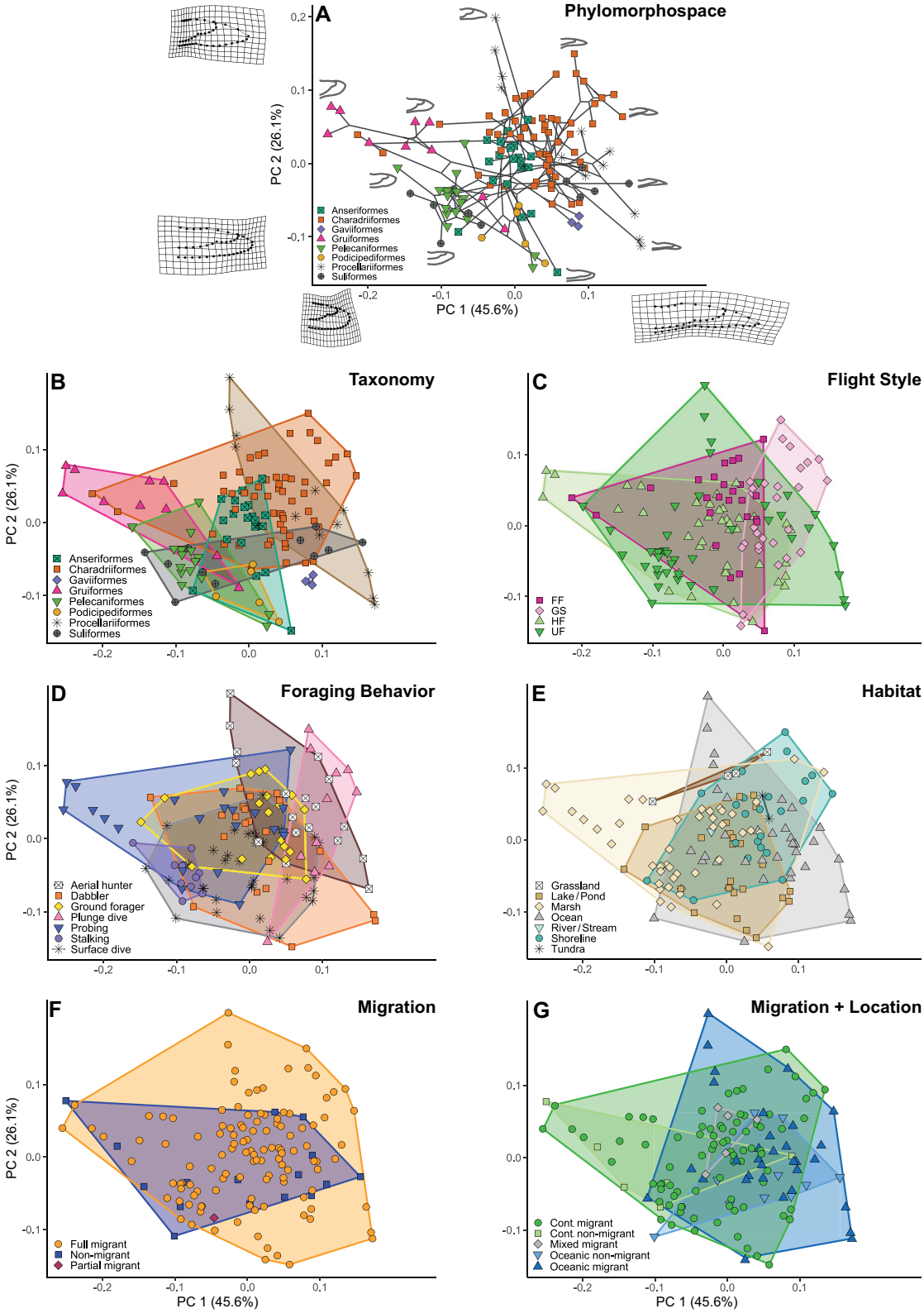

Fig. 6 Whole-wing morphospace based on PCs 1 and 2, 71.7% of total variance. (**A**) Phylomorphospace with warp grids depicting wing shape at extremes of axes and wing shapes of selected specimens. Subsequent morphospaces are colored for (**B**) major clades, (**C**) flight style, (**D**) foraging behavior, (**E**) habitat, (**F**) migration, and (**G**) migration+location. FF, forward/bounding flight; GS, gliding/soaring flight; HF, high-frequency flapping flight; UF, undulating flapping flight. PC scores in Supplementary Table S7. Interactive plot in Supplementary Fig. S7.

distribution of the handwing to armwing areas, as well as the extent to which the dorsal greater coverts cover the wing surface. PC 1 (53.3%) represents the ratio between anterior and posterior armwing areas, with posterior armwing areas generating higher PC 1 values. PC 2 (34.4%) represents the change in relative wingtip area, with smaller wingtip areas generating higher PC 2 values.

Taxonomy provides the strongest separation between groups within WA morphospace. Anseriformes, Gruiformes, Pelecaniformes, and Podicipediformes compose the central cluster (Fig. 7A and B). Charadriiformes are present in the central cluster but also extend into areas of higher (gulls and terns) and lower (a couple jacanas) PC 1 values. Suliformes are split between average and low PC 1 values. Procellariiformes and Gaviiformes tend to have high PC 1 values. There is no major pattern in shape space with regard to flight style, although undulating flappers expand to fill the morphospace (Fig. 7C). Considering foraging, aerial hunters have larger anterior than posterior wings with a range of wingtip sizes (Fig. 7D). Some surface divers and a few probers have large posterior WAs, a wing shape feature not observed in birds characterized by other foraging behaviors. Ocean-dwelling birds tend to have the widest range in morphospace (Fig. 7E). The WAs of other habitats largely overlap, although marsh-dwelling birds with small anterior and large posterior WAs cluster together. Full migrants tend to have greater coverage of morphospace than nonmigrants (Fig. 7F). Oceanic migrants tend to have larger anterior than posterior wings and exhibit a range of wingtip sizes (Fig. 7G). Most categories (except mixed migrant) have representatives with larger posterior than anterior WAs.

Handwing morphospace

Handwing morphospace shows some clustering among the variables (Fig. 8). PC 1 (69.0% of the variation) represents wing tip shape, and PC 2 (15.7% of the variation) records the location of the tip of the first secondary flight feather in relation to the wrist (inclined distally or proximally) and the curvature of the primary flight feathers (straight or curved trailing edge).

Phylogenetically, many of the same trends in the whole-wing morphospace are repeated in handwing morphospace (Fig. 8A and B). Gruiformes and Pelecaniformes tend to have lower PC 1 values, Anseriformes average, and Procellariiformes high PC 1 values. Charadriifromes shows the greatest range in handwing morphospace, and two suliform clusters are on either side of the plot with both high and low PC 1 values. For flight style, forward/bounding flapping flight, and gliding/soaring birds overlap very little, though they overlap with the high-frequency flapping and undulating flapping birds (Fig. 8C). There is a lot of overlap within foraging behavior, aerial hunters, and plunge divers tend toward the right, and probing birds occupy the largest area of morphospace, and are the only ones expanding into the area with low PC 1 and PC 2 values (Fig. 8D). Foraging behavior has a significant relationship with handwing morphospace (phylo-MANOVA: Wilks statistic = 0.369, corrected $P = 0.032$, Supplementary Table S11). Habitat morphospace does not differentiate clusters. Unlike the other habitats, marsh-dwelling birds expand toward low PC 1 and PC 2 values. Habitat also shows a weakly significant relationship with handwing morphospace (phylo-MANOVA: Wilks statistic = 0.571, corrected $P = 0.061$, Supplementary Table S11). There is little difference in migratory versus nonmigratory birds in wing morphospace (Fig. 8F). Oceanic birds tend to have more pointed handwings than continental birds, which occupy a greater range in morphospace (Fig. 8G).

Convergence in waterbird wing shape

When tested within a phylogenetic framework, wing shapes in waterbirds converged at statistically significant levels multiple times. We found significant convergence in whole-wing phylomorphospace among groups of waterbirds with high and with low wing ARs, among clusters of waterbirds with similar foraging behaviors and habitats as well as clusters with a variety of foraging behaviors and habitats (Table 2).

Most of the groups in Table 2 (circled in Fig. 9) had significant C1 convergence in wing shape, indicating that the maximum phylogenetic distance represented by the clusters was greater than expected under the Brownian motion model of evolution. The larger groups (1–3) also featured highly significant C5 values, a statistic indicating that the selected organisms invaded that area of morphospace a greater number of times than would be expected under the Brownian motion model of evolution.

Overall, most groups tested here resulted in significant convergence in wing shape in multiple regions of morphospace. Clusters of species that occupied the regions of morphospace and share similar foraging behaviors and/or habitats had significant convergence (Groups 1, 2, 3, 6, and 12). Regions with clusters of species featuring different foraging behaviors and habitats were also significantly

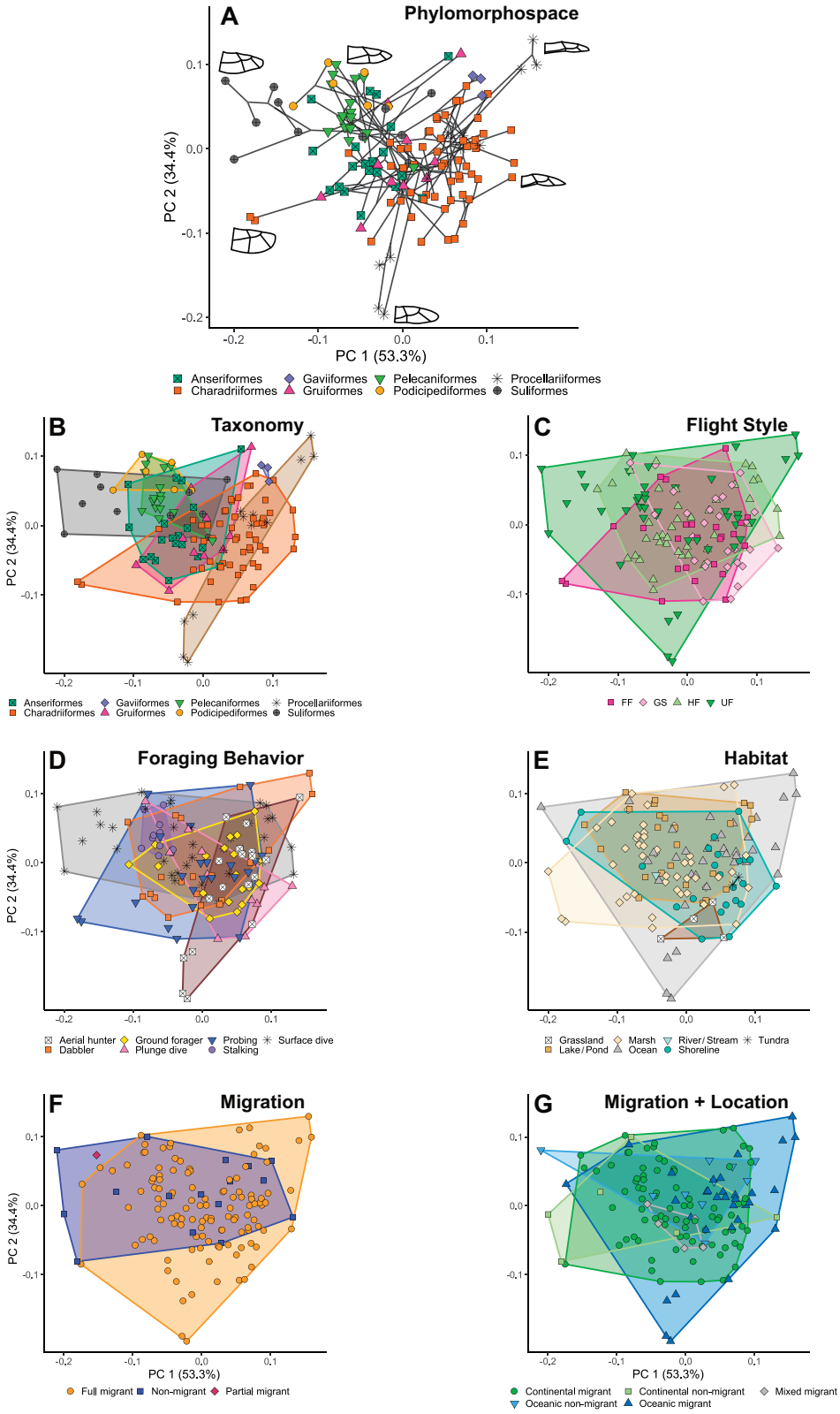

Fig. 7 Wing-area morphospace based on PCs 1 and 2. (**A**) Phylomorphospace with icons depicting extremes of morphospace and WA distributions of selected specimens. Subsequent morphospaces are colored for (**B**) major clades, (**C**) flight style, (**D**) foraging behavior, (**E**) habitat, (**F**) migration, and (**G**) migration+location. PC scores available in Supplementary Table S9. Interactive plot in Supplementary Fig. S8.

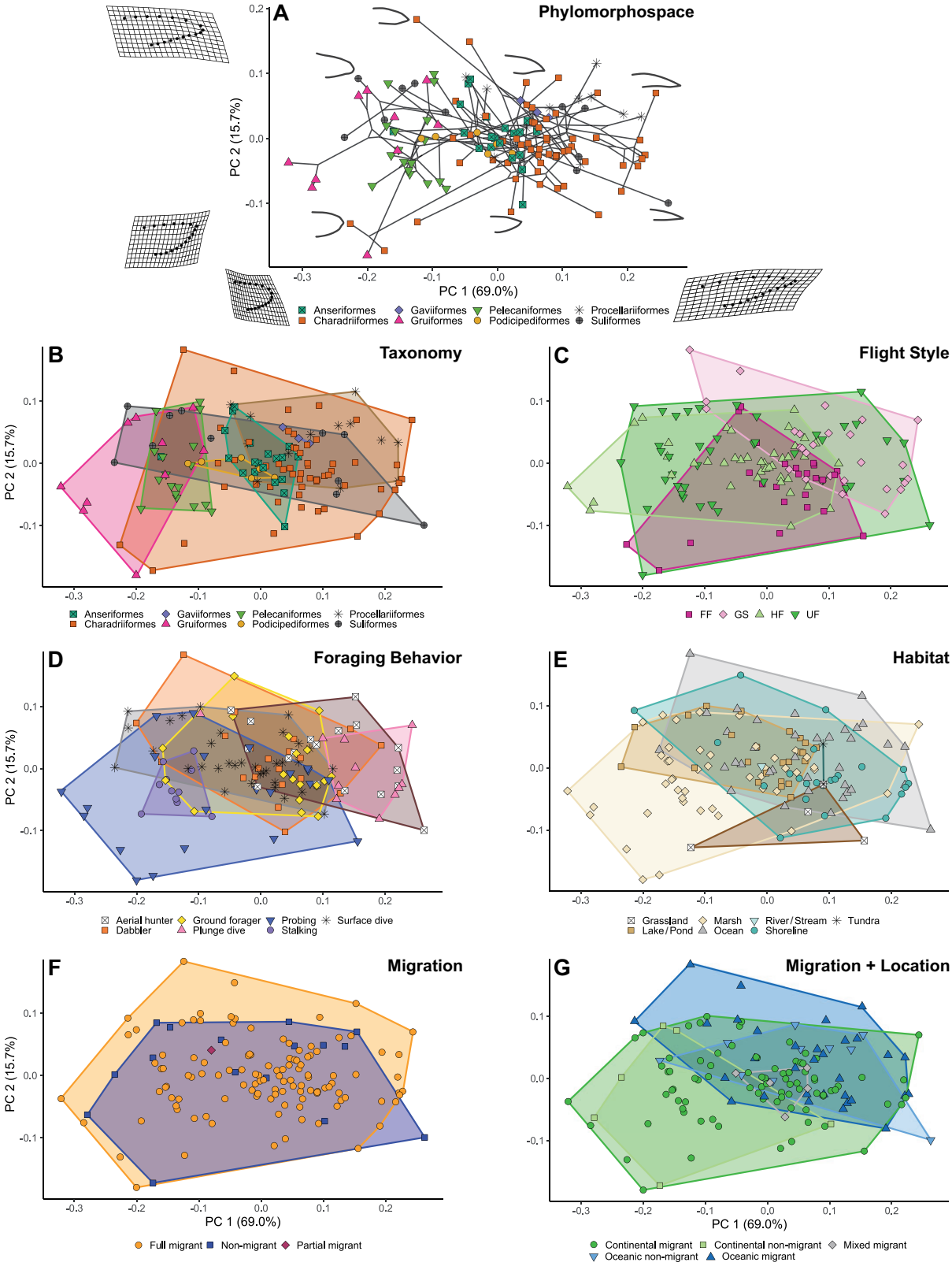

Fig. 8 Handwing morphospace based on PCs 1 and 2. (**A**) Phylomorphospace with warp grids depicting extremes of axes and handwing outlines from selected specimens. Subsequent morphospaces are colored for (**B**) major clades, (**C**) flight style, (**D**) foraging behavior, (**E**) habitat, (**F**) migration, and (**G**) migration+location. PC scores available in Supplementary Table S10. Interactive plot in Supplementary Fig. S9.

Table 2 Convergence testing in the 11 groups of waterbirds circled in Fig. 9

	C1		C5	
Group no.	Obs. C	*P*-value	Obs. C	*P*-value
1	0.625	<0.001	6	<0.001
2	0.458	<0.001	10	0.009
3	0.625	<0.001	6	<0.001
4	0.489	<0.001	—	—
5	0.501	<0.001	—	—
6	0.554	<0.001	—	—
7	0.335	0.018	—	—
8	0.495	0.011	—	—
9	0.340	0.053	—	—
10	0.080	0.385	—	—
11	0.458	0.011	—	—
12	0.391	0.047	—	—

C1 represents the amount of convergence in wing shape within a given area of morphospace (1 = high, 0 = low) and whether this value is significant given the phylogenetic relationships of the group. C5 was restricted to clusters of >5 species and calculates the number of times lineages represented by the selected cluster invaded the area of morphospace and whether that number is significant with relation to the group's phylogenetic relationships.

Group 1: *Aramus guarauna*, *Jacana jacana*, *Jacana spinosa*, *Rallus elegans*, *R. limicola*, and *R. longirostris*; Group 2: *Alca torda*, *B. marmoratus*, *C. monocerata*, *F. glacialis*, *Gavia immer*, *Gavia pacifica*, *Gavia stellata*, *L. marinus*, *Sula dactylatra*, *Sula leucogaster*, and *Sula sula*; Group 3: *Aechmophorus clarkia*, *Dendrocygna bicolor*, *Egretta rufescens*, *P. auritus*, *P. carbo*, and *Podilymbus podiceps*; Group 4: *A. occidentalis*, *B. bernicla*, *P. erythrorhynchos*, *P. occidentalis*, and *P. grisegena*; Group 5: *Aethia cristatella*, *Cygnus buccinator*, *Cygnus columbianus*, *Podiceps auritus*, and *Podiceps nigricollis*; Group 6: *Fregata minor*, *Pterodroma externa*, *Puffinus pacificus*, *Sterna elegans*; Group 7: *A. valisineria*, *B. clangula*, and *P. urinatrix*; Group 8: *C. vociferus*, *O. furcata*; Group 9: *Arenaria melanocephala* and *Clangula hyemalis*; Group 10: *Anhinga anhinga* and *Bubulcus ibis*; Group 11: *Aethia psittacula* and *Branta Canadensis*; Group 12: *C. monocerata* and *Sula sula*.

convergent (Groups 4, 5, 7, 8, and 11) We also located a few pairs that were close in morphospace, but were phylogenetically close enough such that they were not significant in terms of evolutionary convergence (Groups 9 and 10): a ground-foraging turnstone and a surface-diving duck have 34.0% convergence on medium AR wings with a curved leading edge and pointed wings (Group 9: C1 $P = 0.053$; Table 2 and Fig. 9), and a surface-diving darter and a ground-foraging egret have 8.0% convergence on medium AR wings with pointed wingtips and a curved leading edge (Group 10: C1 $P = 0.385$; Table 2 and Fig. 9).

Discussion

The wings of waterbirds are highly diverse in size and shape. They show a broad range when scored for important functional metrics that characterize their functional diversity and evolutionary history. The central conclusion of this study is that important wing metrics such as aspect ratio (AR), wing area (WA), and wing loading (WL) are significantly associated with the trophic ecology and specific habitat traits in waterbird taxa. We also conclude that migratory behavior is not strongly correlated with wing shape in waterbirds from 3 major avian clades, despite a general correlation between handwing index (HWI) and migratory behavior among birds (Dawideit et al. 2009; Sheard et al. 2020). Finally, we have identified multiple regions of phylomorphospace showing convergence in waterbird wing shape. Thus, particular wing shapes appear to be well-suited for survival and reproduction in coastal and aquatic birds.

Trends in waterbird wing shape and ecology

Wing aspect ratio (AR), a frequently used functional metric when studying flight function (Greenewalt 1962; Norberg 1990), is measured as a single- or double-wing variable, the latter 2 times the value of the former metric and calculated from the square of total wingspan tip-to-tip divided by the sum of the area of both wings (Walker and Westneat 2002). The single-wing AR range among waterbirds (1.8–5.8) is similar to that in other broad-based avian datasets, such as Baliga et al. (2019; AR 1.7–5.4) and Wang and Clarke (2014; AR 2.5–8.1) for wider phylogenetic samples of birds, and those of bats (AR 2.2–4.3; Luo et al. 2019), insects (2.3–8.0; Bhat et al. 2019) and even fishes with flapping underwater flight (AR 1.9–4.3; Thorsen and Westneat 2005). The waterbird ecotypes with the highest ARs are aerial hunters and plunge divers, while those with the lowest AR are the probers. Both procellariiforms and suliforms exhibit a wide range of ARs for a wide range of ecological strategies. Most procellariiforms are ocean-dwelling aerial hunters. They are characterized by a broad range in AR and whole-wing shape space to accommodate a range of locomotor demands on the wing. Suliformes, in contrast, is divided into two distinct clusters, one with wings of medium AR (surface-diving cormorants) and another with wings of high AR (plunge-diving gannets). Procellariiforms exhibit a variety of wing shapes for a given foraging behavior, whereas suliforms have two distinct foraging behaviors and two disparate and extreme areas of wing shape space.

AR slope identifies procellariiforms as having the greatest range in wing shape change along the length of the wing. Some procellariiform wings (petrels)

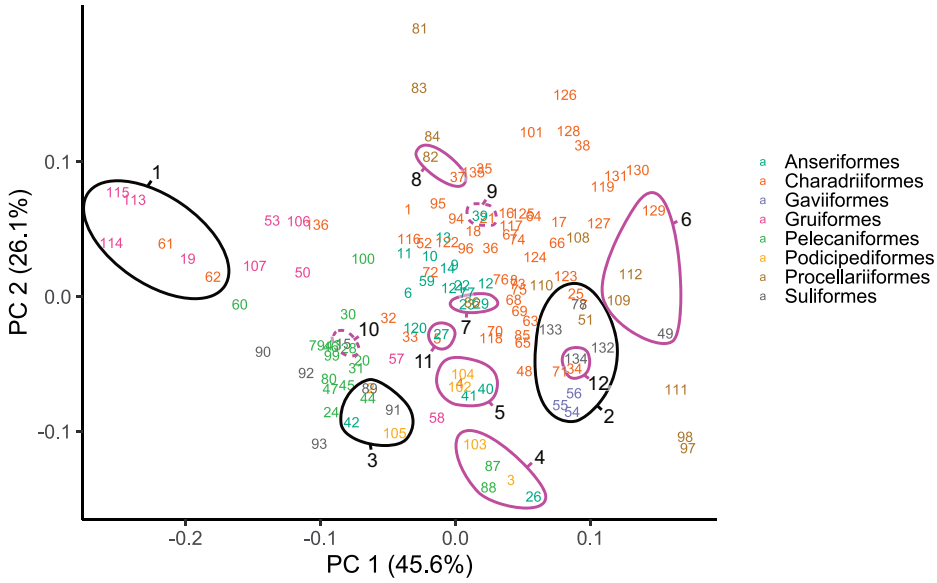

Fig. 9 Testing wing shape convergence within whole-wing morphospace. Colored numbers refer to index of bird species in Supplementary Table S1. Large black numbers refer to group number in Table 2. Black lines indicate larger clusters for convergence testing with C1 and C5, magenta lines indicate smaller clusters for convergence testing with C1. Solid lines indicate significant results, dotted lines indicate insignificant results.

taper much faster than others (albatrosses), which may be related to the specific aerodynamic requirements for different foraging behaviors (aerial hunting versus dabbling). Most other waterbird clades have a small range of AR slope (excluding charadriiform outliers), suggesting that wing taper is a relatively conservative trait in most birds.

Although wing area is the denominator in calculating AR, wing area can be plotted separately. Waterbirds that spend a lot of time flapping (either forward/bounding or high-frequency) have a narrow range of lesser WA, suggesting that smaller wings may be an adaptation for less stressful, repetitive movement. Gliding/soaring birds and undulating flappers have a higher average and range of WA s, underscoring the importance in higher WA and its variation. WA did not differ significantly between gliding/soaring waterbirds and those with undulating flight, and so wingbeat frequency may have less influence over the WA. No specific WA seems optimal for any particular variable, as WA morphospace overlap among variables is substantial. As an example, procellariiforms occupy a very localized region of WA space, which may be the result of the constraints from aerial hunting or from the long bouts of flight required by their oceanic habitat (Warham 1977). On the other hand, the brent goose (Anseriformes: *Branta bernicla*) and sandhill crane (Gruiformes: *Grus canadensis*), which are relatively large birds with long necks that remain extended in flight and travel long distances during migration (Cornell Lab of Ornithology 2015), seem to converge on WA distributions at the top of the WA morphospace (Fig. 7).

Wing loading (WL) is another key parameter yielding insight into the structure and function of wings for flight (Vágási et al. 2016). WL is not tied to a particular wing shape (Supplementary Fig. S10), but rather to the functional demands of the bird. Within a study examining European species, some birds are found to have a low WL that optimizes cost of transport for long distances, whereas other birds have high WL that optimizes speed at the cost of energy efficiency (Vágási et al. 2016). The birds with the highest wing loadings in our waterbird dataset are ducks, loons, and grebes, birds that forage by dabbling and surface diving in lakes/ponds and use high-frequency flapping to get aloft. Loons and grebes are diving birds that have reduced skeletal pneumaticity to increase skeletal density (O'Connor 2009), which in turn increases WL during flight. In contrast, birds that glide and soar have greater skeletal pneumaticity (O'Connor 2009; Smith 2012), reducing body mass and thus WL.

Wing kinematics and wing morphing during flight affects WL (Taylor et al. 2012; Harvey et al. 2019), an important frontier in flight biomechanics. Although presented for uniformity in a single outstretched pose, avian wings have a number of components that may be adjusted during flight. Wing

shape changes at different flight speeds (Lentink et al. 2007; Tobalske 2007). Feathers spread farther apart at slower flight speeds, increasing WA and vice versa (Tobalske 2007). If one assumes a given bird has a constant body mass, the foregoing necessarily means that WL must vary with flight speed.In our study, wing shape is static as in the studies we have extensively cited (Lockwood et al. 1998; Wang and Clarke 2015; Pigot et al. 2020). How wing shape varies during flight across birds is an intriguing question for future research.

Wing shape and migration

Most of the birds we sampled (120 species, 88%) are regarded as full migrants; only 15 species are logged as nonmigrants and 1 as a partial migrant. We could not distinguish any patterns in wing shape that would distinguish migratory versus nonmigratory waterbirds at this scale. The combination variable migration+location, however, shows weak significance with respect to handwing index (HWI), which is commonly used for wingtip shape (Wilks statistic = 7.278, $P = 0.0510$). The relationship between migratory behavior, morphology, and physiology is complex (Piersma et al. 2005). Migratory patterns are known to vary within genera and sometimes within species (Berthold and Terrill 1991; Lockwood et al. 1998; Fernández and Lank 2007). For example, the rail genus *Rallus* includes the nonmigrant *Rallus longirostris* as well as the full migrants *Rallus elegans* and *R. limicola*. Likewise, the cormorant genus *Phalacrocorax* includes the nonmigrants *Phalacrocorax brasilianus* and *Phalacrocorax urile*, the partial migrant (some populations migrate, some do not) *P. carbo*, and the full migrants *Phalacrocorax auritus* and *Phalacrocorax pelagicus*. Despite stark differences in migratory behavior, these birds occupy the same region of morphospace (Fig. 6).

Many aspects of avian biology and behavior influence wing shape, introducing some plasticity in shape at all taxonomic levels. For example, the wing shape of western sandpipers (*Calidris mauri*) varies depending on sex and maturity (Fernández and Lank 2007). Females migrate longer distances than males, and males have to perform aerial displays to attract the females. Therefore, the female wing is longer and more pointed than the wing in males. For rapid escape, immature sandpipers require shorter, rounder wings than adults. Two species of the finch genus *Carduelis* exhibit different wing shapes, the insular nonmigrant Corsican finch (*C. corsicanus* = *C. citrinella corsicanus*) with more rounded wings than the migrant citril finch (*C. citrinella* = *C. citrinella citrinella*) from the mainland (Förschler et al. 2008; Gill et al. 2020). Although the wing shape differences between these finches match expectations given their migratory patterns, their daily locomotor needs may also explain this difference; the insular *C. corsicanus* must navigate dense foliage compared to its mainland counterpart (Förschler et al. 2008). Among our rail species in the genus *Rallus*, *R. longirostris* and *R. elegans* are similar in size and wing shape, but the former is nonmigratory and the latter migratory (Cornell Lab of Ornithology 2015; BirdLife International 2020). Some birds alter migratory habits over the course of a few generations (Berthold and Terrill 1991). Our results suggest that migratory behavior is one factor among many that influence wing shape as shown in previous studies (Mönkkönen 1995; Baldwin et al. 2010; Huber et al. 2017).

Evolutionary convergence across phylomorphospace

Four general patterns emerge from our morphometric analysis of wing form across birds. First, phylomorphospace plots indicate the presence of a significant phylogenetic component to many aspects of avian wing morphology (Wang and Clarke 2015; Pigot et al. 2020). Thus, clade membership has some predictive value with regard to wing morphology.

Second, most sampled waterbirds cluster in the centroid of distribution for a range of wing metrics. These waterbirds are characterized by a wide range of locomotor, foraging and migratory behaviors, and ecological habitats. Thus, the sweet spot of wing morphospace among waterbirds is occupied by distantly related taxa with disparate functional, behavioral, and ecological traits. Similar to limb morphospace for disparate clades among rodents, outliers in morphospace are limited to extreme morphologies, such as the limbs of fossorial taxa (Hedrick et al. 2020).

Third, a few avian subgroups did plot in relatively extreme wing morphospace, such as the low AR wings of the probing jacanas and rails and the high AR wings of aerial and plunge diving specialists (terns, gannets, and petrels). In these cases, therefore, wing morphology seems strongly linked to their specialized lifestyles, unlike the vast majority of birds occupying the center of morphospace where aerodynamic factors rather than disparate functional and ecological traits govern wing morphology.

Finally, these conclusions highlight the prevalence of convergence in wing morphospace across

Table 3 "Group 4" waterbirds showing convergence in wing morphospace

Species	Taxonomy	Flight style	Foraging behavior	Habitat	Body mass (kg)	AR	WL ($N \cdot m^{-2}$)
Pelecanus erythrorhynchos	Pel.	GS	Surface dive	Lake/pond	4.970	2.1	87.4
Pelecanus occidentalis	Pel.	GS	Plunge dive	Ocean	3.702	2.4	81.8
Aechmophorus occidentalis	Pod.	HF	Surface dive	Lake/pond	1.429	1.6	203.5
Podiceps grisegena	Pod.	HF	Surface dive	Lake/pond	1.023	3.3	167.2
Branta bernicla	Ans.	FF	Dabble	Marsh	1.370	1.7	153.7

Pod., Podicipediformes; Ans., Anseriformes; Pel., Pelecaniformes.

waterbirds. We identified and tested 12 likely instances of wing shape convergence. The selected clusters included areas with high and low AR wings in pairs and larger groups of taxa and sampled the majority of waterbird phylomorphospace. Ten out of 12 of these groups were highly significant examples of convergence on similar wing shape from distant ancestral starting points (Table 2). Convergence in form among flapping appendages is a major evolutionary pattern in organisms as diverse as birds (Norberg 1986, 1990), bats (Norberg 1986), insects (Strauss 1990), and bony fish (Aiello et al. 2017).

Several of the convergent clusters share foraging behavior or habitat, supporting the hypothesis that there is an optimal wing shape for a given behavior or habitat. Jacanas (Charadriiformes), rails, and the limpkin (Gruiformes) show an average of 62.5% convergence on very low AR wings with rounded wingtips and a slightly larger handwing than armwing (Group 1: C1 $P = 0$; Fig. 9 and Table 2). The species in this cluster transitioned into this space 6 times, significantly more than would be expected by chance (C5 $P = 0$; Table 2). Loons (Gaviiformes) also appear to converge in wing shape with gannets and boobies (Suliformes: Sulidae) (Group 2: Fig. 9 and Table 2) in a region of morphospace shared with a procellariiform (*Fulmarus glacialis*) and a few charadriiforms (*Brachyramphus marmoratus*, *Cerorhinca monocerata*, and *Larus marinus*). This group averages 45.8% convergence on high AR wings with somewhat pointy wingtips, a relatively straight edge and a relatively larger armwing than handwing (C1 $P = 0$). The species in this cluster transitioned into this morphospace 10 times, significantly more than would be expected by chance (C5 $P = 0.009$; Table 2). Within this cluster, the charadriiform, the rhinoceros auklet (*C. monocerata*), and red-footed booby (*Sula sula*) share 39.1% convergence (Group 12: C1 $P = 0.047$; Table 2 and Fig. 9). Another cluster of waterbirds with high AR wings (Group 6: frigatebird, petrel, shearwater, and tern) averaged 55.4% convergence (C1 $P = 0$; Fig. 9).

Other convergent clusters are composed of waterbirds with a range of behaviors and habitats, suggesting wing shapes may be employed in multiple behaviors and habitats with only extreme wing shapes tied to extreme behaviors and habitats. For example, two pelecaniforms (*Pelecanus erythrorhynchos* and *Pelecanus occidentalis*), an anseriform (*B. bernicla*), and two podicipediforms (*Aechmophorus occidentalis* and *Podiceps grisegena*) averaged 45.8% convergence on medium AR wings with rounded wingtips and a much larger armwing than handwing (Group 4: C1 $P = 0$; Table 2 and Fig. 9). Swans, an auklet, and grebes averaged 50.1% convergence on medium AR wings with a straighter leading edge, a slightly rounded wingtip, and slightly larger armwings than handwings (Group 5: C1 $P = 0$; Table 2 and Fig. 9). Two anseriforms (*Aythya valisineria* and *Bucephala clangula*) and a procellariiform (*Pelecanoides urinatrix*) averaged 33.5% convergence on medium AR wings with slightly pointed wingtips and a comparatively similar handwing to armwing (Group 7: C1 $P = 0.018$; Table 2 and Fig. 9). A ground-foraging charadriiform (*Charadrius vociferus*) and an aerial-hunting procellariiform (*Oceanodroma furcata)* averaged 49.5% convergence on medium AR wings with very pointed tips and a much larger handwing than armwing (Group 8: C1 $P = 0.011$; Table 2 and Fig. 9).

Group 4 waterbirds (Table 3), which include two pelicans (*Pelecanus)*, two grebes (*A. occidentalis* and *P. grisegena)* and the brent goose (*B. bernicla*), differ markedly in behavior, habitat and overall morphology. This disparate cluster of species is an example of convergence with no basis in the ecological or functional variables examined in this study. The pelicans glide and soar, the grebes use high-frequency flapping, and the brent goose employs forward/bounding flapping flight. Regarding foraging behaviors, the pelicans plunge (*P. occidentalis*) and surface dive (*P. erythrorhynchos*), the grebes surface dive, and the brent goose dabbles. Regarding habitats, pelicans live near lakes and ponds (*P. erythrorhynchos*) and oceans (*P. occidentalis*), the grebes live near lakes and ponds, and the brent goose prefers marshes. In size they range from medium to the high end of body mass range (1–5 kg). Birds with similar WL are

present across wing morphospace (Supplementary Fig. S8).

Very few regions of whole-wing morphospace are truly dominated by a specific behavior or habitat. The highest AR wings characterize oceanic birds that glide and soar, and the lowest AR wings are found in birds that hunt from the ground in more enclosed habitats. In between these extremes, wing shapes have evolved convergently and are used in a variety of behaviors and habitats. It appears waterbirds are broadly adapted to more open habitats with wing shapes that serve multiple lifestyles and at least partially overlap in morphospace with birds in terrestrial habitats (Wang and Clarke 2015).

Conclusions

Avian wings are appendages of great functional importance to birds and show great shape diversity, ranging from those of high to low AR and those with rounded or pointed wingtips. Yet, it has proved challenging to find significant and regular correlation across birds between wing shape and flight style or various ecological traits. In this study, we examined multiple functional and ecological variables, determining that wing shape and foraging behavior are significantly correlated in waterbirds. In contrast, flight style, habitat, and migratory status are not correlated, although combining migratory status and location (continental versus oceanic) shows a weak correlation. Phylogenetic signal, as shown in previous studies, is prevalent, such that wing shape within clades exhibited similarity. Nevertheless, the central morphospace for most traits shows broad overlap of unrelated taxa. This work highlights the complexity in correlating wing shape to aerodynamic performance as well as a number of nonaerodynamic variables. The current study and its forerunners are based on static (spread) wing shape, leaving open for future research considering wing shape as a dynamic variable that changes with flight speed.

Acknowledgments

We thank the University of Puget Sound's Slater Museum of Natural History for access to bird wing images via the online Wing and Tail Image Collection. Special thanks to Aaron Olsen, Jacqueline Lungmus, Ryan Felice, Andrew George, Matthew Kaufman, and Manabu Sakamoto for discussions of geometric morphometrics, comparative methods, and R techniques. This manuscript was greatly improved in review by John Bates, Michael Coates, and the anonymous reviewers. We also thank Daniel Vidal, Jordan Gônet, and Romain Cottereau for the Spanish and French abstracts.

Funding

This work was supported by the US Department of Education's Graduate Assistance in Areas of National Need in Integrative Neuromechanics fellowship [grant number: P200A150077] to S.L.B., a generous donation from SC Johnson to P.C.S., and National Science Foundation grant DEB 1541547 to M.W.W.

Declaration of competing interest

The authors declare no competing or conflicting interests.

Data availability statement

The wing image data underlying this article were provided by the Wing and Tail Image Collection hosted by the University of Puget Sound's Slater Museum of Natural History at https://digitalcollections.pugetsound.edu/digital/collection/slaterwing, and the derived data are available in the article and in its online supplementary material.

Supplementary Data

Supplementary Data available at *IOB* online.

References

Adams DC, Collyer ML, Kaliontzopoulou A. 2021. Geomorph: software for geometric morphometric analyses. R package version 3.2.2. (https://cran.r-project.org/package=geomorph) (accessed July 21, 2020).

Aiello BR, Westneat MW, Hale ME. 2017. Mechanosensation is evolutionarily tuned to locomotor mechanics. Proc Natl Acad Sci USA 114:4459–64.

Alexander D. 2015. On the wing: insects, pterosaurs, birds, bats and the evolution of animal flight. New York (NY): Oxford University Press.

Baldwin MW, Winkler H, Organ CL, Helm B. 2010. Wing pointedness associated with migratory distance in common-garden and comparative studies of stonechats (*Saxicola torquata*). J Evol Biol 23:1050–63.

Baliga VB, Szabo I, Altshuler DL. 2019. Range of motion in the avian wing is strongly associated with flight behavior and body mass. Sci Adv 5:eaaw6670.

Barr A. 2017. ggphylomorpho. GitHub Ggphylomorpho. (https://github.com/wabarr/ggphylomorpho/) (accessed March 3, 2020).

Berthold P, Terrill SB. 1991. Recent advances in studies of bird migration. Annu Rev Ecol Syst 22:357–78.

Bhat SS, Zhao J, Sheridan J, Hourigan K, Thompson MC. 2019. Aspect ratio studies on insect wings. Phys Fluid 31:121301.

BirdLife International. 2020. IUCN red lst for birds. http://www.birdlife.org/ (accessed May 14, 2020).

Brewer ML, Hertel F. 2007. Wing morphology and flight behavior of pelecaniform seabirds. J Morphol 268:866–77.
Claramunt S, Derryberry EP, Remsen JV, Brumfield RT. 2012. High dispersal ability inhibits speciation in a continental radiation of passerine birds. Proc R Soc B Biol Sci 279:1567–74.
Collyer ML, Adams DC. 2018. RRPP: an R package for fitting linear models to high-dimensional data using residual randomization. Methods Ecol Evol 9:1772–9.
Collyer ML, Adams DC. 2020. RRPP: linear model evaluation with randomized residuals in a permutation procedure. R package version 0.5.2. (https://cran.r-project.org/package=RRPP) (accessed July 22, 2020).
Combes SA, Daniel TL. 2001. Shape, flapping and flexion: wing and fin design for forward flight. J Exp Biol 204:2073–85.
Cornell Lab of Ornithology. 2015. All about birds. https://www.allaboutbirds.org/ (accessed May 15, 2019).
Da Vinci L. 1505. The codex on the flight of birds. Turin, Italy. https://airandspace.si.edu/exhibitions/codex/codex.cfm#page-1 (accessed May 6, 2020).
Dawideit BA, Phillimore AB, Laube I, Leisler B, Böhning-Gaese K. 2009. Ecomorphological predictors of natal dispersal distances in birds. J Anim Ecol 78:388–95.
Drummond AJ, Rambaut A. 2007. BEAST: Bayesian evolutionary analysis by sampling trees. BMC Evol Biol 7:214.
Dunning. JB.Jr. 2007. CRC handbook of avian body masses. 2nd ed. New York (NY): CRC Press.
Ehrlich P, Dobkin DS, Wheye D. 1988. The birder's handbook: a field guide to the natural history of North American birds. New York (NY): Simon and Schuster, Inc.
Ellington CP. 1984. The aerodynamics of hovering insect flight. II. Morphological parameters. Philos Trans R Soc Lond B Biol Sci 305:17–40.
Fernández G, Lank DB. 2007. Variation in the wing morphology of western sandpipers (*Calidris mauri*) in relation to sex, age class, and annual cycle. The Auk 124:1037–46. doi:10.1093/auk/124.3.1037.
Förschler MI, Siebenrock KH, Coppack T. 2008. Corsican finches have less pointed wings than their migratory congeners on the mainland. Vie Milieu 58:277–81.
Gill F, Donsker D, Rasmussen P. 2020. IOC world bird list (v10.1). Finches Euphonias longspurs Thrush-Tanager. http://worldbirdnames.org/bow/finches/ (accessed July 17, 2020).
Greenewalt CH. 1962. Dimensional relationships for flying animals. Smithson Misc Collect 144: 1–46.
Greenewalt CH. 1975. The flight of birds: the significant dimensions, their departure from the requirements for dimensional similarity, and the effect on flight aerodynamics of that departure. Trans Am Philos Soc 65:1–67.
Hackett SJ, Kimball RT, Reddy S, Bowie RCK, Braun EL, Braun MJ, Chojnowski JL, Cox WA, Han KL, Harshman J, et al. 2008. A phylogenomic study of birds reveals their evolutionary history. Science 320:1763–8.
Hansen JR. 2003. The bird is on the wing: aerodynamics and the progress of the American airplane. College Station (TX): Texas A&M University Press.
Harmon LJ, Weir JT, Brock CD, Glor RE, Challenger W. 2008. GEIGER: investigating evolutionary radiations. Bioinformatics 24:129–31.
Hartman FA. 1961. Locomotor mechanisms of birds. Smithson Misc Collect 143: 1–91.
Harvey C, Baliga VB, Lavoie P, Altshuler DL. 2019. Wing morphing allows gulls to modulate static pitch stability during gliding. J R Soc Interface 16:20180641.
Hedrick BP, Dickson BV, Dumont ER, Pierce SE. 2020. The evolutionary diversity of locomotor innovation in rodents is not linked to proximal limb morphology. Sci Rep 10:11.
Higham TE. 2007. The integration of locomotion and prey capture in vertebrates: morphology, behavior, and performance. Int Comp Biol 47:82–95.
Huber GH, Turbek SP, Bostwick KS, Safran RJ. 2017. Comparative analysis reveals migratory swallows (Hirundinidae) have less pointed wings than residents. Biol J Linn Soc 120:228–35.
Jetz W, Thomas GH, Joy JB, Hartman K, Mooers AO. 2012. The global diversity of birds in space and time. Nature 491:444–8.
Kipp FA. 1959. Der Handflügel-Index als flugbiologisches Maß. Vogelwarte 20:77–86.
Lentink D, Biewener AA. 2010. Nature-inspired flight—beyond the leap. Bioinspir Biomim 5:040201.
Lentink D, Müller UK, Stamhuis EJ, de Kat R, van Gestel W, Veldhuis LLM, Henningsson P, Hedenström A, Videler JJ, van Leeuwen JL. 2007. How swifts control their glide performance with morphing wings. Nature 446:1082–5.
Lockwood R, Swaddle JP, Rayner JMV. 1998. Avian wingtip shape reconsidered: wingtip shape indices and morphological adaptations to migration. J Avian Biol 29:273–92.
Luo B, Santana SE, Pang Y, Wang M, Xiao Y, Feng J. 2019. Wing morphology predicts geographic range size in vespertilionid bats. Sci Rep 9:4526.
Martin-Silverstone E, Habib MB, Hone DWE. 2020. Volant fossil vertebrates: potential for bioinspired flight technology. Trends Ecol Evol 35:618–29.http://www.sciencedirect.com/science/article/pii/S016953472030080X (accessed April 10, 2020).
Minias P, Meissner W, Włodarczyk R, Ożarowska A, Piasecka A, Kaczmarek K, Janiszewski T. 2015. Wing shape and migration in shorebirds: a comparative study. Ibis 157:528–35.
Mönkkönen M. 1995. Do migrant birds have more pointed wings: a comparative study. Evol Ecol 9:520–8.
Mosimann JE. 1970. Size allometry: Size and shape variables with characterizations of the lognormal and generalized gamma distributions. J Am Stat Assoc 65:930–45.
Mulvihill RS, Chandler CR. 1990. The relationship between wing shape and differential migration in the dark-eyed junco. Auk 107:490–9.
Myers P, Espinosa R, Parr CS, Jones T, Hammond GS, Dewey TA. 2020. The animal diversity web (online). University of Michigan www.animaldiversity.org (accessed Sept 10, 2019).
Norberg UM. 1986. Evolutionary convergence in foraging niche and flight morphology in insectivorous aerial-hawking birds and bats. Ornis Scand Scand J Ornithol 17:253–60.
Norberg UM. 1990. Vertebrate flight: mechanics, physiology, morphology, ecology and evolution. Berlin, Heidelberg: Springer (Zoophysiology).
Norberg UM. 1995. How a long tail and changes in mass and wing shape affect the cost for flight in animals. Funct Ecol 9:48–54.

Norberg UM, Rayner JMV. 1987. Ecological morphology and flight in bats (Mammalia; Chiroptera): wing adaptations, flight performance, foraging strategy and echolocation. Philos Trans R Soc B Biol Sci 316:335–427.

O'Connor PM. 2009. Evolution of archosaurian body plans: skeletal adaptations of an air-sac-based breathing apparatus in birds and other archosaurs. J Exp Zool Part Ecol Genet Physiol 311:629–46.

Olsen AM, Haber A. 2017. StereoMorph: stereo camera calibration and reconstruction manual. Version 1.6.1. (https://CRAN.R-project.org/package=StereoMorph) (accessed July 26, 2019).

Olsen AM, Westneat MW. 2015. StereoMorph: an R package for the collection of 3D landmarks and curves using a stereo camera set-up. Meth Ecol Evol 6:351–6.

Paradis E, Schliep K. 2019. ape 5.0: an environment for modern phylogenetics and evolutionary analyses in R. Bioinformatics 35:526–8.

Pennycuick CJ. 2008. Modelling the flying bird. Amsterdam, Netherlands: Elsevier.

Piersma T, Pérez-Tris J, Mouritsen H, Bauchinger U, Bairlein F. 2005. Is there a "migratory syndrome" common to all migrant birds? Ann N Y Acad Sci 1046:282–93.

Pigot AL, Sheard C, Miller ET, Bregman TP, Freeman BG, Roll U, Seddon N, Trisos CH, Weeks BC, Tobias JA. 2020. Macroevolutionary convergence connects morphological form to ecological function in birds. Nat Ecol Evol 4:230–9.

Price SA, Friedman ST, Corn KA, Martinez CM, Larouche O, Wainwright PC. 2019. Building a body shape morphospace of teleostean fishes. Integr Comp Biol 59:716–30.

Prum RO, Berv JS, Dornburg A, Field DJ, Townsend JP, Lemmon EM, Lemmon AR. 2015. A comprehensive phylogeny of birds (Aves) using targeted next-generation DNA sequencing. Nature 526:569–73.

R Core Team. 2020. R: a language and environment for statistical computing. Version 3.6.3. Vienna, Austria: R Foundation for Statistical Computing.

Revell LJ. 2012. phytools: an R package for phylogenetic comparative biology (and other things). Methods Ecol Evol 3:217–23.

Sheard C, Neate-Clegg MHC, Alioravainen N, Jones SEI, Vincent C, MacGregor HEA, Bregman TP, Claramunt S, Tobias JA. 2020. Ecological drivers of global gradients in avian dispersal inferred from wing morphology. Nature Commun 11: 1–9.

Sibley D. 2018. Wing basics by David Sibley. BirdWatching.. https://www.birdwatchingdaily.com/birds/david-sibleys-id-toolkit/wing-basics-by-david-sibley/ (accessed March 2, 2020).

Sievert C. 2020. Interactive web-based data visualization with R, plotly, and shiny. Chapman and Hall/CRC. https://plotly-r.com. (accessed March 8, 2021).

Slater Museum of Natural History. 2011. Wing & Tail Image Collection. http://digitalcollections.pugetsound.edu/cdm/landingpage/collection/slaterwing (accessed May 8, 2017).

Smith ND. 2012. Body mass and foraging ecology predict evolutionary patterns of skeletal pneumaticity in the diverse "waterbird" clade. Evolution 66:1059–78.

Stayton CT. 2015. The definition, recognition, and interpretation of convergent evolution, and two new measures for quantifying and assessing the significance of convergence. Evolution 69:2140–53.

Strauss RE. 1990. Patterns of quantitative variation in lepidopteran wing morphology: the convergent groups Heliconiinae and Ithomiinae (Papilionoidea: Nymphalidae). Evolution 44:86–103.

Swaddle JP, Lockwood R. 2003. Wingtip shape and flight performance in the European Starling *Sturnus vulgaris*. Ibis 145:457–64.

Taylor GK, Carruthers AC, Hubel TY, Walker SM. 2012. Wing morphing in insects, birds and bats: mechanism and function. In: Valasek J, editor. Morphing aerospace vehicles and structures. Chichester, UK: John Wiley & Sons, Ltd. p. 13–40.

Thorsen DH, Westneat MW. 2005. Diversity of pectoral fin structure and function in fishes with labriform propulsion. J Morphol 263:133–50.

Tobalske BW. 2007. Biomechanics of bird flight. J Exp Biol 210:3135–46.

Tokita M, Matsushita H, Asakura Y. 2020. Developmental mechanisms underlying webbed foot morphological diversity in waterbirds. Sci Rep 10:8028.

Vágási CI, Pap PL, Vincze O, Osváth G, Erritzøe J, Møller AP. 2016. Morphological adaptations to migration in birds. Evol Biol 43:48–59.

Viscor G, Fuster JF. 1987. Relationships between morphological parameters in birds with different flying habits. Comp Biochem Physiol A Physiol 87:231–49.

Walker JA, Westneat MW. 2002. Performance limits of labriform propulsion and correlates with fin shape and motion. J Exp Biol 205:177–87.

Wang X, Clarke JA. 2014. Phylogeny and forelimb disparity in waterbirds. Evolution 68:2847–60.

Wang X, Clarke JA. 2015. The evolution of avian wing shape and previously unrecognized trends in covert feathering. Proc R Soc B 282:20151935.

Warham J. 1977. Wing loadings, wing shapes, and flight capabilities of procellariiformes. N Z J Zool 4:73–83.

Webb PW. 1984. Body form, locomotion and foraging in aquatic vertebrates. Am Zool 24:107–20.

Wickham H. 2016. ggplot2: elegant graphics for data analysis. R package version 3.3.2. New York (NY): Springer-Verlag New York.

Resumen La forma del ala tiene un papel crítico en el vuelo de las aves y otros voladores activos, y se ha comprobado que se correlaciona con la eficiencia del vuelo, la distancia migratoria y la biomecánica en la generación de sustentación durante el vuelo. La forma de las alas de las aves y la mecánica del vuelo también están relacionadas con las estrategias de búsqueda de alimento y elección de hábitat. Nuestro propósito es determinar si la forma del ala se correlaciona con varias características funcionales y ecológicas en aves acuáticas, un grupo funcional y ecológicamente diverso que comparten un hábito costero y acuático. Se utilizó morfometría geométrica en alas extendidas de una selección de aves acuáticas para buscar patrones evolutivos entre la morfología del ala y estrategia de alimentación, hábitat y patrones migratorios. Se ha encontrado evidencia robusta de evolución convergente de morfologías de ala con mayor o menor alargamiento en varios clados. El comportamiento de búsqueda de alimento también tiene correlaciones evolutivas consistentes con la morfología del ala. Sin embargo, el hábitat, tipo de migración y tipo de vuelo no muestran una correlación significativa con la morfología del ala en aves acuáticas. Aunque la forma del ala es crítica para la función del vuelo aéreo, su relación con el hábitat o demandas locomotoras periódicas como la migración son complejas.